Food and Chemical Toxicology 130 (2019) 207–218

Contents lists available at ScienceDirect

Food and Chemical Toxicology

journal homepage: www.elsevier.com/locate/foodchemtox

Pharmacophore studies of 1, 3, 4-oxadiazole nucleus: Lead compounds as α-glucosidase inhibitors

Haroon Khan[a,*], Muhammad Zafar[a], Seema Patel[b], SM Mukarrum Shah[c], Anupam Bishayee[d]

[a] Department of Pharmacy, Abdul Wali Khan University Mardan, 23200, Pakistan
[b] Bioinformatics and Medical Informatics Research Center, San Diego State University, San Diego, 92182, USA
[c] Department of Pharmacy, University of Swabi, Pakistan
[d] Lake Erie College of Osteopathic Medicine, Bradenton, FL, 34211, USA

ARTICLE INFO

Keywords:
α-glucosidase enzyme
Pharmacophore modeling
Molecular docking
Pharmacophore-based virtual screening

ABSTRACT

α-glucosidase inhibition is a rational approach in the effective management of type 2 diabetes. Several inhibitors of this enzyme class are in clinical use, but are riddled with efficacy, potency and safety challenges. For this reason, new effective α-glucosidase inhibitors are under investigation. Compounds with 1, 3, 4-oxadiazole nucleus have shown preclinical efficacy as α-glucosidase inhibitors and as anti-inflammatory agents. Moreover, 1, 3, 4-oxadiazoles also play important role in pesticide chemistry, polymer science, and they are considered as the building blocks in the production of new molecular agents for bioactive molecules. In the present study, computational analyses were carried out for various 1,3,4-oxadiazole (which were divided into BF2 & BF3 series); the most active compound was taken as a potent inhibitor, and pharmacophore were formed from that compound, followed by validation against a test database. The pharmacophore-based virtual screening was performed and, by successive eliminations, six compounds of different interactions with the significant amino acid residues were selected as the lead compounds. It is concluded that these six compounds with 1, 3, 4-oxadiazoles nucleus might be used as promising drug candidates in α-glucosidase inactivation and thus we recommend further in vitro and in vivo pharmacological and safety studies.

1. Introduction

Diabetes is a metabolic disease characterized by hyperglycemia, reduced glucose tolerance, and insulin-releasing abnormalities. Diabetes mellitus or type 2 diabetes is one of the most common chronic endocrine, inflammatory diseases, which occurs when the levels of insulin produced by pancreas is inadequate, or when the body is incapable of utilizing insulin properly (Kato et al., 2012; Zakir et al., 2019). Data projections reveal that as of 2015, about 415 million people are suffering from diabetes all over the world (Abbas et al., 2017; Association, 2010; Sultan et al., 2016a). Among the several types of diabetes, type 2 diabetes is the most leading form, responsible for almost 90% of all cases worldwide (Sultan et al., 2016a, 2016b). The pathogenesis of type 2 diabetes is complex and comprises an interaction between genetic vulnerability and environmental factors, especially the intake of such diets that results in obesity together with physical inactivity (Khattak and Khan, 2018). Due to pollution and a sedentary, lifestyles, type 2 diabetes is emerging as one of the most rapidly-developing, non-communicable disease (Kallemeijn et al., 2014; Zafar et al., 2016). If not managed, it can lead to diabetic nephropathy and neuropathy. Diabetes is a state of oxidative stress, and it affects cell homeostasis, extracellular matrix composition, mitochondrial functions. Pancreas is prone to ischemia due to hypoxia and acidosis, which gradually loses insulin secretory function (Wang et al., 2016; Yin et al., 2014). People suffering from type 2 diabetes need to inject themselves with insulin and to follow a careful diet and exercise regimen (Sultan et al., 2016b). The existing drugs, such as metformin, when used for prolonged period, generate side effects, including abdominal discomfort, anorexia, diarrhea, hepatic and renal impairment (Domekouo et al., 2016; Nathan et al., 2006; Virally et al., 2007). α-glucosidase (EC 3.2.1.20), an enzyme hydrolyzing α-glucosidic linkage, is targeted to manage type 2 diabetes. Inhibition of this enzyme delays digestion of dietary carbohydrates, lowering postprandial blood glucose level. In this regard, several research groups have been working on the discovery of new effective α-glucosidase inhibitors, which can be used as therapeutic agents for the suppression of metabolic disorders, such as hyperglycemia, obesity, and non-insulin-dependent type 2 diabetes mellitus (Kim, 2015; Zafar et al., 2016). Heterocyclic compounds

* Corresponding author.
E-mail address: hkdr2006@gmail.com (H. Khan).

https://doi.org/10.1016/j.fct.2019.05.006
Received 14 January 2019; Received in revised form 30 March 2019; Accepted 4 May 2019
Available online 23 May 2019

containing the five-membered oxadiazole nucleus possess a diversity of useful biological effects (Singh and Jangra, 2010).

In particular, compounds bearing the 1, 3, 4-oxadiazole nucleus are known to have unique anti-edema and anti-inflammatory activities (Amir and Kumar, 2007; Narayana et al., 2005; Omar et al., 1996). So, 1, 3, 4-oxadiazoles are playing significant role in medicinal chemistry, pesticide chemistry, polymer science and they are considered to be the building blocks in the production of new molecular systems for active biological molecules (Reynisson et al., 2009). Most of the 1, 3, 4-oxadiazoles exhibited a significant biological activity, such as antimicrobial (Jha et al., 2010; Manjunatha et al., 2010), anti-Human Deficiency Virus (HIV) (El-Emam et al., 2004), antitubercular (Küçükgüzel et al., 2002), antimalarial (Chandrakantha et al., 2010), analgesic (Akhter et al., 2009), anti-inflammatory (Padmavathi et al., 2010), among others (Singh et al., 2011). The drugs like nitrofuran antibacterial furamizole, HIV-integrase inhibitor raltagravir, and antihypertensive agents tiodazosin and nesapidil are based on the 1,3,4-oxadiazole (Somani and Shirodkar, 2011). The oxadiazole pharmacophore have significant properties (ability to undergo electrophillic substitution, nucleophilic substitution, thermal and photochemical) that influences the ability of a drug to reach the target (bioavailability) by transmembrane diffusion and shows potent antimicrobial activity (Somani and Shirodkar, 2011; Testa et al., 2000). Inspired by the above evidences (Deep et al., 2010; Kumar and Verma, 2009), its relevance in diabetes mitigation was pursued. In the present study, the biological activity of the synthesized oxadiazole compounds were found out. Among the synthetic compounds, the most active compound is deemed to be a potent inhibitor and pharmacophore was formed from that compound and then validated by a test database. Then further pharmacophore based virtual screening was conducted to find the novel, potential and other structurally-diverse compounds, which might be used to inhibit the α-glucosidase enzyme.

The pharmacophore models are important tools for the virtual screening (Yang et al., 2012) and to rapidly search large databases for drug candidates with better therapeutic action. The virtual screening has been used effectively to predict novel inhibitor compounds in the case of the *α*-glucosidase (Derksen et al., 2006; Lu et al., 2006; Scarsi et al., 2007). In the current study, we used pharmacophore-based virtual screening method by docking appropriate compounds (hits) against α-glucosidase enzyme, to identify druggable candidates (Reynisson et al., 2009). Virtual screening is the chemo-informatic methods, involving the use of high performance computing to examine the large database of the compounds to find out the possible leads (Shaikh et al., 2008). The main objective of the present study is to generate homology model of the α-glucosidase enzyme, to develop a valid pharmacophore model, to develop novel and potent inhibitors for this diabetogenic enzyme.

2. Materials and method

2.1. Ligand preparation

The structures of the synthesized compounds were generated by using the Chembio-Office 2010–12. Then all these compounds were saved in mol file for the purpose to open in molecular operating environment (MOE) Further, the compounds were energy minimized via MOE, using default parameters.

2.2. Protein preparation

The modeled structure of the target protein was 3D protonated and then energy minimization was performed by using the MOE software with default parameters.

2.3. Molecular docking

Molecular docking was performed via MOE-dock with most of the default tools with the aim to find the binding interaction of the ligand with the target protein. The ligand was docked into the binding site of predicted homology model of the α-glucosidase by means of MOE-Dock module (v. 2010.11), and for each ligand 10 conformations were generated. The top ranked conformation of each ligand was used for detailed study of binding mode.

2.4. Complex-based pharmacophore model generation and validation

Among the synthesized compounds, the docked conformer of the most active compound interacting with the active residues of the binding pocket of the target protein, was used to generate the complex-based pharmacophore model. In MOE pharmacophore constructing tool is employed and used for the construction and visualization of the 3D pharmacophore for structural data of receptor-ligand complex. On the basis of binding interactions, main chemical features were recognized, which were observed in the protein-ligand complex for the generation of pharmacophore model. A total of five important features including two hydrogen bond acceptors (Acc), one Don&Acc, and two Hyd|Aro were generated in the resulting pharmacophore model, by using the default parameters of MOE. These five features (F1, F2, F3, F4, and F5), were chosen as essential. The generated pharmacophore model was validated by a test database of ten known inhibitors of α-glucosidase (Kashtoh et al., 2014; Sattar et al., 2016; Shyma et al.). All compounds of the test database were screened at the five-featured complex-based pharmacophore, and their mapping modes were analyzed.

2.5. Pharmacophore-based database screening

The validated pharmacophore model is used as three-dimensional query in the *in silico* screening of hits of numerous chemical natures. Using the software MOE 2010–11, pharmacophore based virtual screening was performed against the ChemBridge database (Wadood et al., 2012). Such type of virtual screening has two main purposes; first, the selective detection of compounds with known inhibitory activity validates the quality of the generated pharmacophore model, and second, finding novel potent drug-like candidates offers options for further assessment (Kurogi and Guner, 2001). As a result of VS, 37 structurally diverse hits are retrieved from ChemBridge database showing a good and better five features, fit to produce pharmacophore model. Following the Lipinski's rule of five (Barret, 2018), each hit ligand properties were examined, to study the druggable properties of the retrieved hits. By the observed criteria of the above rule, for further progression 33 hits were selected.

2.6. Molecular docking

All the retrieved hits were docked into the binding pocket of α-glucosidase to further refine the hit compounds. For molecular docking study, several docking programs are available. In this study, we used the docking protocol implemented in MOE 2010–11 as a docking program (Kitchen et al., 2004). For further evaluation, on the basis of docking score, the top poses were selected for further evaluation. The resulting binding interactions between these hits and protein were observed visually using LigPlot implemented in MOE.

2.7. Calculations of the binding affinity and binding energy

To find out the most potential ligands, the binding affinities of the hits with α-glucosidase was predicted with generalized Born / volume integral (GB/VI) contained solvent scheme executed in MOE (Labute, 2008). The non-bonded interaction energies are the generalized Born interaction energy between the ligand and receptor molecule, which

comprises Vander Waals, Coulomb electrostatic interactions and implied solvent interaction energies. The receptor molecules and ligands have strain energies which were not considered. The solvent molecules were unobserved during the calculation. The receptor atoms in the vicinity of the ligand are retained flexible during calculation, while the receptor molecule atoms which are away from the ligand are retained rigid but were focused to the tether restraints which weaken unrefined movement. In the binding pocket, the atoms of the ligand are set free to move. Before an estimation of the binding affinity, an energy minimization of the binding pocket in α-glucosidase enzyme-ligand complex was done. After energy minimization, for each hit, the binding affinity is calculated and reported in the unit of the Kcal/Mol.

3. Results

3.1. Complex-based pharmacophore model generation and validation

One interesting application of complex-based pharmacophore model is to define interaction points that results in the improvement of binding affinity and increasing selectivity. MOE software was used in generating a pharmacophore model from α-glucosidase-ligand complex. For the building of the pharmacophore model, the essential chemical features were recognized and this was performed by keeping the binding interactions in the protein-ligand complex through LigPlot, in MOE. By using the default parameters of MOE, five important features were generated in the given pharmacophore model, which contains two hydrogen bond acceptors (Acc), one Don&Acc and two Hyd|Aro. F1 was Don&Acc and represented by red color, F2 and F5 was Hyd|Aro and was represented by purple color, F3 and F4 was Acc and represented by cyan color shown in Fig. 1.

The Don&Acc feature F1 was developed on the hydroxyl moiety of the inhibitor. F2 and F5 features were Hyd|Aro and developed on the benzene and pyridine moiety, respectively, of the ligand. F3 and F4 features were Acc and developed on the oxygen double bonded with carbon atom and nitrogen atom of the 1, 3, 4-oxadiazole moiety respectively, all these features interact with the important amino acid residues. The F1, F2, F3, F4 and F5 features were chosen as essential features (Kashtoh et al., 2014; Niaz et al., 2015; Sattar et al., 2016; Shyma et al.). The three-dimensional structure of the inhibitors in the test database was generated by using builder tool in MOE and then through energy minimization algorithm *i.e.* Gradient: 0.05, and Force Field: MMFF94X. The test database compounds were then screened on five features complex-based pharmacophore and the mapping modes of these compounds were examined. All active compounds were screened against the generated pharmacophore and mapping the five features of generated pharmacophore model. The result of this test database revealed that the generated pharmacophore model is accurate.

3.2. Pharmacophore-based database screening

The pharmacophore model was validated and used for screening compounds from the ChemBridge database. Those compounds that have similar features were screened, the whole process was performed to identify the new structural poses that accomplish the recognized criteria of the pharmacophore model. It is an easy approach for the discovery of potent and novel compounds in research projects. Then through virtual screening from the ChemBridge database, 37 structurally-different hits were retrieved, showing that five essential features were well-fitted for generating pharmacophore model. According to the Lipinski's rule of five, the druggable properties of the retrieved hits were checked Lipinski's rule of five states that a drug candidate must be lesser than 500 Da in molecular weight, the hydrogen bond acceptors lesser than ten, hydrogen bond donors lesser than five and the value of log p should be less than five (Lipinski et al., 2012). Finally, by applying the Lipinski's rule of five, we obtained the 33 hits, which can be used for further evaluation by using the molecular docking technique.

3.3. Molecular docking

Molecular Docking was done for all the retrieved hit compounds which were obtained primarily, with the binding site of the α-glucosidase enzyme, for the purpose of finding more refine hit compounds and this was carried out by the docking protocol MOE. All the initial hits are docked into the binding pocket of the α-glucosidase enzyme and this was carried out by using the similar docking protocol. By means of the default parameters of MOE, for each ligand 10 conformations are allowed to be saved. All the docked compounds have different conformations. So, the top ranked conformations were permitted to be saved in a separate database. In top ranked conformations, according to the docking scores, the best 16 poses out of the initially selected 33 hits, were chosen for further assessment. With the help of LigPlot in MOE, the interactions of the 16 hits with the α-glucosidase binding pocket residues GLN66, MET69, TYR71 ASP106, ILE109, HIS111, ASN152, ASN153, TRP154, LYS155, SER156, PHE157, PHE158, LEU174, ARG175, GLN181, ARG212, ILE213, THR215, ILE230, LYS233, LYS236, LEU237, GLN238, HIS239, TRP242, VAL274, GLU276, PHE300, PHE311, ARG312, TYR313, ASN347, ASP349, GLN350, ASP408, ASN412, LEU437, and ARG439 were observed. Ten out of 16 compounds showed important interactions with the target protein residues, so they were selected for further evaluations of binding affinity and binding energy.

3.4. Binding energy and binding affinity calculations

The criteria for the selection of the potential compounds are those possessing binding affinity and binding energy equivalent to the

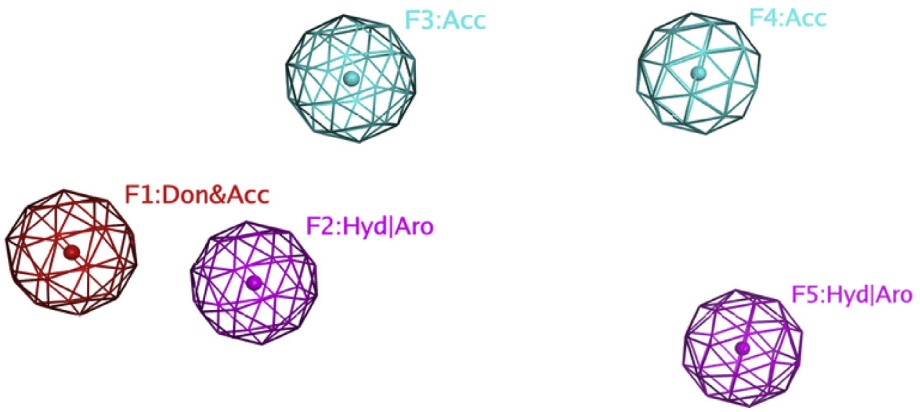

Fig. 1. Three-dimensional pharmacophoric features generated from the complex structure of α-glucosidase and BF2-57.

Table 1
ChemBridge database ID, Docking Scores (S), binding energies Kcal/mol, binding affinities Kcal/mol and drug like properties of the retrieved hit compounds.

S. No	Chembridge ID	Docking score (S)	Binding energy (Kcal/mol)	Binding affinity (Kcal/mol)	Drug like properties
1	57484801	−15.8941	−35.089	−11.2946	**MW**.387.528, **Log P.** 2.067, **Don**.1, **Acc.**5, **Log S.** −2.8916
2	23224339	−15.0034	−26.463	−10.4331	**MW**.486.637, **Log P.** 4.090, **Don**.3, **Acc.**5, **Log S.** −4.8273
3	27519658	−14.2341	−20.774	−10.3952	**MW**.474.564, **Log P.** 4.120, **Don**.1, **Acc.**5, **Log S.** −2.9294
4	65892932	−13.8971	−19.621	−9.7974	**MW**.352.398, **Log P.** 1.795, **Don**.1, **Acc.**5, **Log S.** −1.6999
5	13601161	−12.0934	−18.672	−8.0640	**MW**.390.357, **Log P.** 3.923, **Don**.2, **Acc.**4, **Log S.** −4.6476
6	54006709	−11.2365	−18.775	−8.0026	**MW**.391.492, **Log P.** 2.467, **Don**.2, **Acc.**4, **Log S.** −2.8650

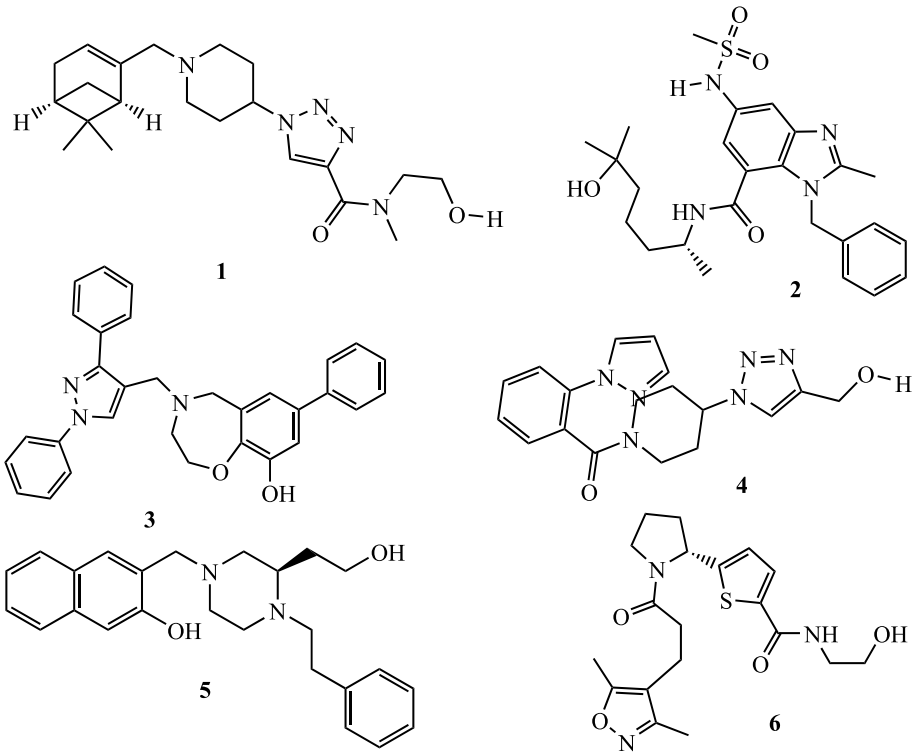

Fig. 2. The two-dimensional structures of the 6 retrieved hit compounds, which may have the potential to be a novel inhibitor.

calculated value for reference ligand in the complex structure. So, the binding affinities of all of the 10 compounds containing the ligand of the complex structure were calculated with GB/VI through MOE, in order to recognize the most favorable ligands. After performing energy minimization for each hit, the binding affinity was measured in units of the Kcal/Mol. Based on the measurements, only 6 compounds were chosen among the 10 compounds shown in Table 1. The mapping of the pharmacophore, binding energy, binding affinity, visual prediction and binding mode have shown that 6 lead compounds may act as the structurally-diverse, potent and novel inhibitors of the α-glucosidase enzyme. The 2D structures of the 6 retrieved hit compounds are shown in Fig. 2 (see Table 2).

3.5. Binding interactions of the hit compounds and target protein

In the present investigation, the potent and novel hit compounds were obtained through virtual screening and the resultant hit compounds formed interactions with the target protein α-glucosidase as shown below.

4. Discussion

4.1. Pharmacophore-based virtual screening

Binding interactions of the finally selected retrieved hits from Chembridge database.

As a result of pharmacophore-based virtual screening, finally 6 compounds were selected which possessed good docking scores as well as good interactions with the active residues of the enzyme. Compound **1** have docking score −15.8941, strong binding affinity −11.2946 Kcal/Mol and lower binding energy −35.089. It's binding interactions with the amino acid residues of binding pocket of the enzyme as shown in Fig. 3. This compound formed five polar, two hydrophobic and one arene-arene interaction with the residues of the enzyme. Gly 159 and Asn 412 formed H-bonds with the nitrogen atoms of the triazole moiety. Ser 235 and Ile 416 formed polar interactions with the carbonyl oxygen atom and –OH moiety of the ligand, respectively. Phe 312 made arene-arene linkage with the triazole ring of the compound. Asn 412 and Ile 415 formed hydrophobic interactions with the compound.

From the docking conformation of compound **2**, it was observed to have five polar and one arene-arene interactions as shown in Fig. 4. Arg 312 made H-bond with –OH moiety. His 279 and His 239 formed hydrophilic interactions with the oxygen atoms of the N-methyl methane sulfonamide moiety. Glu 304 made H-bond with the –NH of the N-methyl methane sulfonamide moiety of the ligand. Phe 157 and His 245 was observed having π-π and polar interactions with the 1-methyl-4,5-dihydro-1H-imidazole moiety.

Compound **3** was observed having good interactions with the residues of the target protein as shown in Fig. 5. Gly 159 and Asn 412 made polar contact with –OH moiety of the compound. His 279 formed

Table 2
List of tested of oxadiazol derivatives with structures and molecular weight.

S. #	CODE	STRUCTURE	MW.; g/mol
	BF-II-40	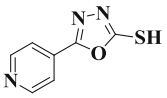 5-(pyridin-4-yl)-1,3,4-oxadiazole-2-thiol	179
	BF-II-46	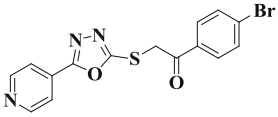 1-(4-bromophenyl)-2-(5-(pyridin-4-yl)-1,3,4-oxadiazol-2-ylthio)ethanone	376
	BF-II-47	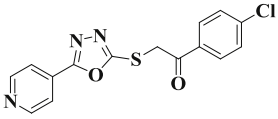 1-(4-chlorophenyl)-2-(5-(pyridin-4-yl)-1,3,4-oxadiazol-2-ylthio)ethanone	331
	BF-II-48	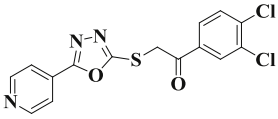 1-(3,4-dichlorophenyl)-2-(5-(pyridin-4-yl)-1,3,4-oxadiazol-2-ylthio)ethanone	365
	BF-II-49	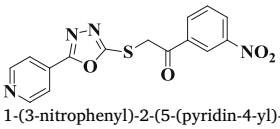 1-(3-nitrophenyl)-2-(5-(pyridin-4-yl)-1,3,4-oxadiazol-2-ylthio)ethanone	342
	BF-II-51	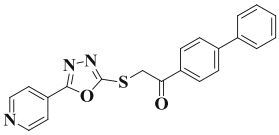 1-(biphenyl-4-yl)-2-(5-(pyridin-4-yl)-1,3,4-oxadiazol-2-ylthio)ethanone	373
	BF-II-52	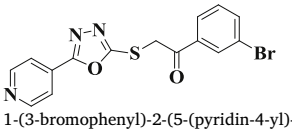 1-(3-bromophenyl)-2-(5-(pyridin-4-yl)-1,3,4-oxadiazol-2-ylthio)ethanone	375
	BF-II-53	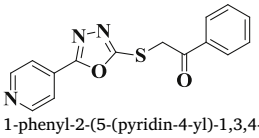 1-phenyl-2-(5-(pyridin-4-yl)-1,3,4-oxadiazol-2-ylthio)ethanone	297
	BF-II-54	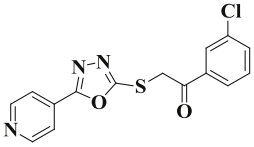 1-(3-chlorophenyl)-2-(5-(pyridin-4-yl)-1,3,4-oxadiazol-2-ylthio)ethanone	331
	BF-II-55	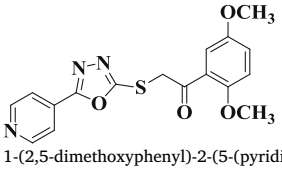 1-(2,5-dimethoxyphenyl)-2-(5-(pyridin-4-yl)-1,3,4-oxadiazol-2-ylthio)ethanone	357

Table 2 (*continued*)

S. #	CODE	STRUCTURE	MW.; g/mol
	BF-II-56	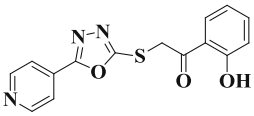 1-(2-hydroxyphenyl)-2-(5-(pyridin-4-yl)-1,3,4-oxadiazol-2-ylthio)ethanone	313
	BF-II-57	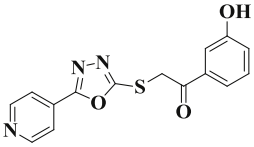 1-(3-hydroxyphenyl)-2-(5-(pyridin-4-yl)-1,3,4-oxadiazol-2-ylthio)ethanone	313.
	BF-II-61	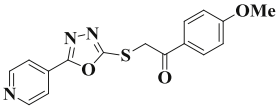 1-(4-methoxyphenyl)-2-(5-(pyridin-4-yl)-1,3,4-oxadiazol-2-ylthio)ethanone	327.
	BF-II-62.	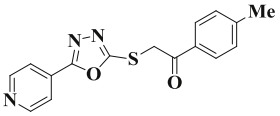 2-(5-(pyridin-4-yl)-1,3,4-oxadiazol-2-ylthio)-1-p-tolylethanone	311.
	BF-II-63	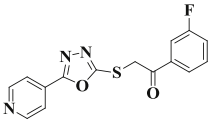 1-(3-fluorophenyl)-2-(5-(pyridin-4-yl)-1,3,4-oxadiazol-2-ylthio)ethanone	315.
	BF-II-64	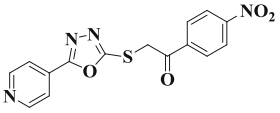 1-(4-nitrophenyl)-2-(5-(pyridin-4-yl)-1,3,4-oxadiazol-2-ylthio)ethanone	342.
	BF-II-73	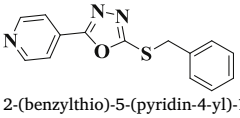 2-(benzylthio)-5-(pyridin-4-yl)-1,3,4-oxadiazole	269.
	BF-II-74	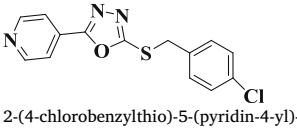 2-(4-chlorobenzylthio)-5-(pyridin-4-yl)-1,3,4-oxadiazole	303.
	BF-II-75	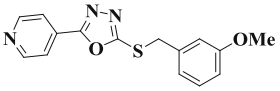 2-(3-methoxybenzylthio)-5-(pyridin-4-yl)-1,3,4-oxadiazole	299.
	BF-II-76	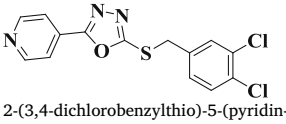 2-(3,4-dichlorobenzylthio)-5-(pyridin-4-yl)-1,3,4-oxadiazole	337.
21.	BF-II-77	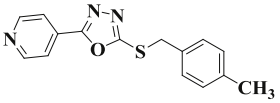 2-(4-methylbenzylthio)-5-(pyridin-4-yl)-1,3,4-oxadiazole	283.

(*continued on next page*)

Table 2 (*continued*)

S. #	CODE	STRUCTURE	MW.; g/mol
22.	BF-II-78	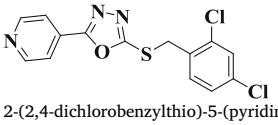 2-(2,4-dichlorobenzylthio)-5-(pyridin-4-yl)-1,3,4-oxadiazole	337.
23.	BF-II-79	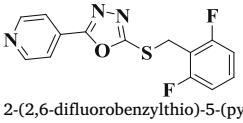 2-(2,6-difluorobenzylthio)-5-(pyridin-4-yl)-1,3,4-oxadiazole	305.
24.	BF-II-82	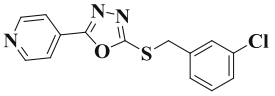 2-(3-chlorobenzylthio)-5-(pyridin-4-yl)-1,3,4-oxadiazole	303.
25.	BF-II-83	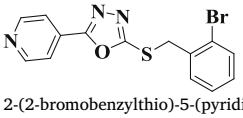 2-(2-bromobenzylthio)-5-(pyridin-4-yl)-1,3,4-oxadiazole	347.
26.	BF-II-84	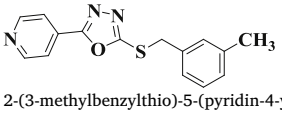 2-(3-methylbenzylthio)-5-(pyridin-4-yl)-1,3,4-oxadiazole	283.
27.	BF-II-85	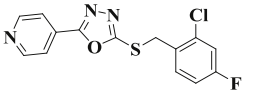 2-(2-chloro-4-fluorobenzylthio)-5-(pyridin-4-yl)-1,3,4-oxadiazole	321.
28.	BF-II-86	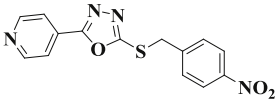 2-(4-nitrobenzylthio)-5-(pyridin-4-yl)-1,3,4-oxadiazole	314.
29.	BF-II-87	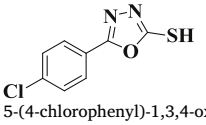 5-(4-chlorophenyl)-1,3,4-oxadiazole-2-thiol	212.
30.	BF-II-88	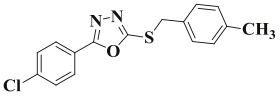 2-(4-chlorophenyl)-5-(4-methylbenzylthio)-1,3,4-oxadiazole	316.
31.	BF-II-89	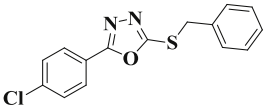 2-(benzylthio)-5-(4-chlorophenyl)-1,3,4-oxadiazole	302.
32.	BF-II-90	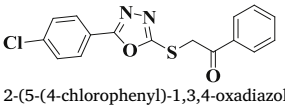 2-(5-(4-chlorophenyl)-1,3,4-oxadiazol-2-ylthio)-1-phenylethanone	330.
33.	BF-II-91	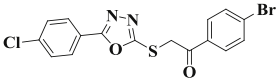 1-(4-bromophenyl)-2-(5-(4-chlorophenyl)-1,3,4-oxadiazol-2-ylthio)ethanone	408.

Table 2 (*continued*)

S. #	CODE	STRUCTURE	MW.; g/mol
34.	BF-II-92	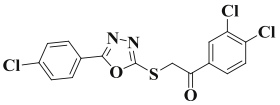 2-(5-(4-chlorophenyl)-1,3,4-oxadiazol-2-ylthio)-1-(3,4-dichlorophenyl)ethanone	398.
35.	BF-II-93	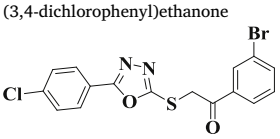 1-(3-bromophenyl)-2-(5-(4-chlorophenyl)-1,3,4-oxadiazol-2-ylthio)ethanone	408.
36.	BF-II-94	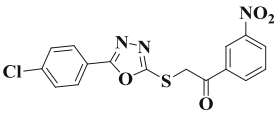 2-(5-(4-chlorophenyl)-1,3,4-oxadiazol-2-ylthio)-1-(3-nitrophenyl)ethanone	375.
37.	BF-II-95	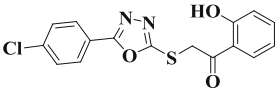 2-(5-(4-chlorophenyl)-1,3,4-oxadiazol-2-ylthio)-1-(2-hydroxyphenyl)ethanone	346.
38.	BF-II-96	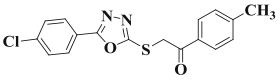 2-(5-(4-chlorophenyl)-1,3,4-oxadiazol-2-ylthio)-1-p-tolylethanone	344.
39.	BF-II-97	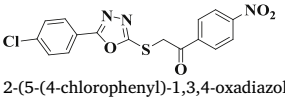 2-(5-(4-chlorophenyl)-1,3,4-oxadiazol-2-ylthio)-1-(4-nitrophenyl)ethanone	375.
40.	BF-II-98	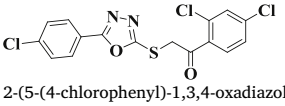 2-(5-(4-chlorophenyl)-1,3,4-oxadiazol-2-ylthio)-1-(2,4-dichlorophenyl)ethanone	398.
41.	BF-II-99	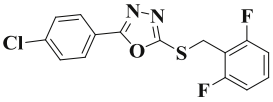 2-(4-chlorophenyl)-5-(2,6-difluorobenzylthio)-1,3,4-oxadiazole	338.
42.	BF-II-100	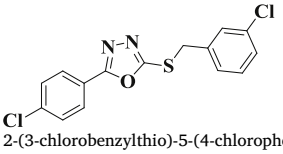 2-(3-chlorobenzylthio)-5-(4-chlorophenyl)-1,3,4-oxadiazole	336.
43.	BF-III-6	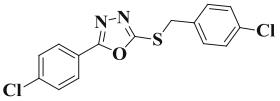 2-(4-chlorobenzylthio)-5-(4-chlorophenyl)-1,3,4-oxadiazole	336.
44.	BF-III-7	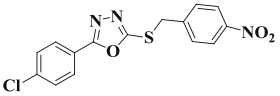 2-(4-chlorophenyl)-5-(4-nitrobenzylthio)-1,3,4-oxadiazole	347.

(*continued on next page*)

Table 2 (*continued*)

S. #	CODE	STRUCTURE	MW.; g/mol
45.	BF-III-8	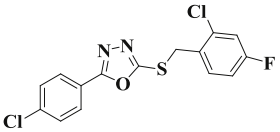 2-(2-chloro-4-fluorobenzylthio)-5-(4-chlorophenyl)-1,3,4-oxadiazole	354.
46.	BF-III-9	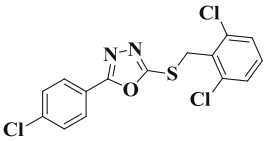 2-(4-chlorophenyl)-5-(2,6-dichlorobenzylthio)-1,3,4-oxadiazole	370.
47.	BF-III-10	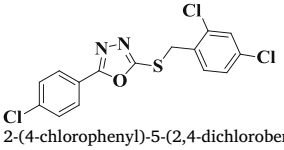 2-(4-chlorophenyl)-5-(2,4-dichlorobenzylthio)-1,3,4-oxadiazole	370.
48.	BF-III-11	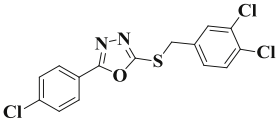 2-(4-chlorophenyl)-5-(3,4-dichlorobenzylthio)-1,3,4-oxadiazole	370.
49.	BF-III-12	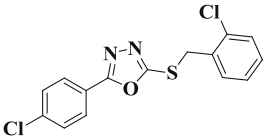 2-(2-chlorobenzylthio)-5-(4-chlorophenyl)-1,3,4-oxadiazole	336.
50.	BF-III-13	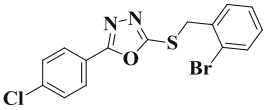 2-(2-bromobenzylthio)-5-(4-chlorophenyl)-1,3,4-oxadiazole	380.
51.	BF-III-14	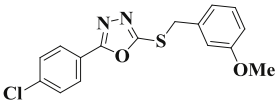 2-(4-chlorophenyl)-5-(3-methoxybenzylthio)-1,3,4-oxadiazole	332.
52.	BF-III-15	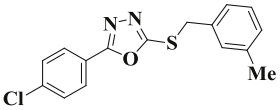 2-(4-chlorophenyl)-5-(3-methylbenzylthio)-1,3,4-oxadiazole	316.
53.	BF-III-17	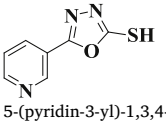 5-(pyridin-3-yl)-1,3,4-oxadiazole-2-thiol	179.
54.	BF-III-18	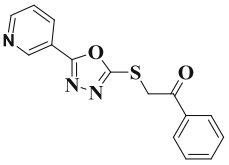 1-phenyl-2-(5-(pyridin-3-yl)-1,3,4-oxadiazol-2-ylthio)ethanone	297.

Table 2 (*continued*)

S. #	CODE	STRUCTURE	MW.; g/mol
55.	BF-III-19	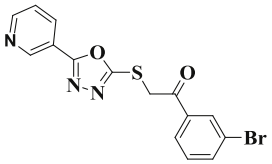 1-(3-bromophenyl)-2-(5-(pyridin-3-yl)-1,3,4-oxadiazol-2-ylthio)ethanone	375.
56.	BF-III-20	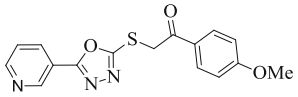 1-(4-methoxyphenyl)-2-(5-(pyridin-3-yl)-1,3,4-oxadiazol-2-ylthio)ethanone	327.
57.	BF-III-21	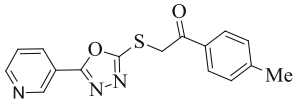 2-(5-(pyridin-3-yl)-1,3,4-oxadiazol-2-ylthio)-1-p-tolylethanone	311.
58.	BF-III-22	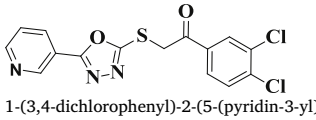 1-(3,4-dichlorophenyl)-2-(5-(pyridin-3-yl)-1,3,4-oxadiazol-2-ylthio)ethanone	365.
59.	BF-III-23	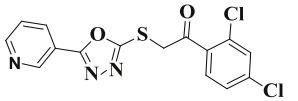 1-(2,4-dichlorophenyl)-2-(5-(pyridin-3-yl)-1,3,4-oxadiazol-2-ylthio)ethanone	365.
60.	BF-III-24	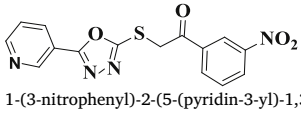 1-(3-nitrophenyl)-2-(5-(pyridin-3-yl)-1,3,4-oxadiazol-2-ylthio)ethanone	342.
61.	BF-III-25	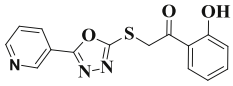 1-(2-hydroxyphenyl)-2-(5-(pyridin-3-yl)-1,3,4-oxadiazol-2-ylthio)ethanone	313.
62.	BF-III-27	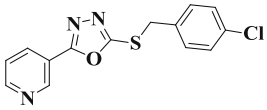 2-(4-chlorobenzylthio)-5-(pyridin-3-yl)-1,3,4-oxadiazole	303.
63.	BF-III-28	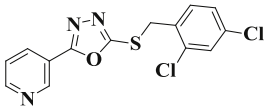 2-(2,4-dichlorobenzylthio)-5-(pyridin-3-yl)-1,3,4-oxadiazole	337.
64.	BF-III-29	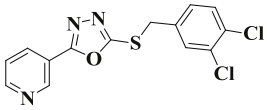 2-(3,4-dichlorobenzylthio)-5-(pyridin-3-yl)-1,3,4-oxadiazole	337.
65.	BF-III-30	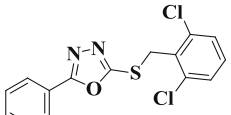 2-(2,6-dichlorobenzylthio)-5-(pyridin-3-yl)-1,3,4-oxadiazole	337.

(*continued on next page*)

Table 2 (*continued*)

S. #	CODE	STRUCTURE	MW.; g/mol
66.	BF-III-31	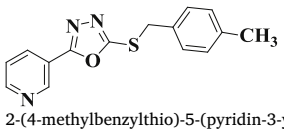 2-(4-methylbenzylthio)-5-(pyridin-3-yl)-1,3,4-oxadiazole	283.
67.	BF-III-32	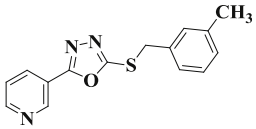 2-(3-methylbenzylthio)-5-(pyridin-3-yl)-1,3,4-oxadiazole	283.
68.	BF-III-34	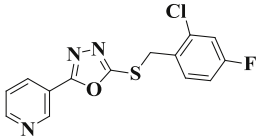 2-(2-chloro-4-fluorobenzylthio)-5-(pyridin-3-yl)-1,3,4-oxadiazole	321.
69.	BF-III-35	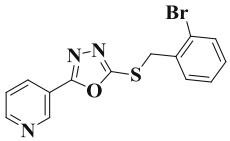 2-(2-bromobenzylthio)-5-(pyridin-3-yl)-1,3,4-oxadiazole	348.
70.	BF-III-36	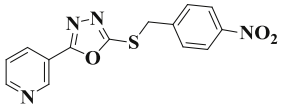 2-(4-nitrobenzylthio)-5-(pyridin-3-yl)-1,3,4-oxadiazole	314.
71.	BF-III-37	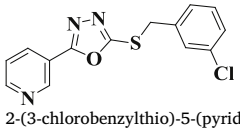 2-(3-chlorobenzylthio)-5-(pyridin-3-yl)-1,3,4-oxadiazole	303.
72.	BF-III-38	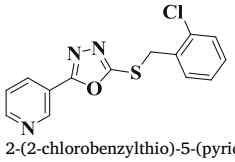 2-(2-chlorobenzylthio)-5-(pyridin-3-yl)-1,3,4-oxadiazole	304.
73.	BF-III-39	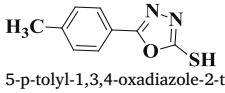 5-p-tolyl-1,3,4-oxadiazole-2-thiol	192.
74.	BF-III-40	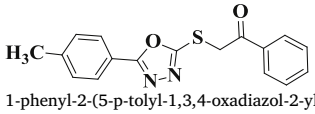 1-phenyl-2-(5-p-tolyl-1,3,4-oxadiazol-2-ylthio) ethanone	310.
75.	BF-III-41	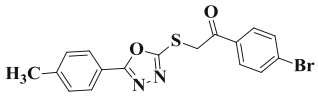 1-(4-bromophenyl)-2-(5-p-tolyl-1,3,4-oxadiazol-2-ylthio)ethanone	388.
76.	BF-III-42	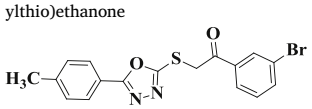 1-(3-bromophenyl)-2-(5-p-tolyl-1,3,4-oxadiazol-2-ylthio)ethanone	388.

Table 2 (*continued*)

S. #	CODE	STRUCTURE	MW.; g/mol
77.	BF-III-43	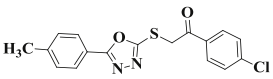 1-(4-chlorophenyl)-2-(5-p-tolyl-1,3,4-oxadiazol-2-ylthio)ethanone	344.
78.	BF-III-44	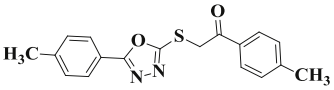 1-p-tolyl-2-(5-p-tolyl-1,3,4-oxadiazol-2-ylthio) ethanone	324.
79.	BF-III-45	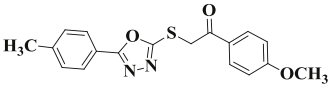 1-(4-methoxyphenyl)-2-(5-p-tolyl-1,3,4-oxadiazol-2-ylthio)ethanone	340.
80.	BF-III-46	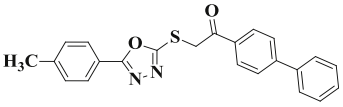 1-(biphenyl-4-yl)-2-(5-p-tolyl-1,3,4-oxadiazol-2-ylthio)ethanone	386.
81.	BF-III-47	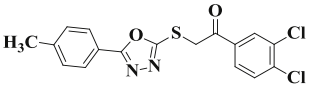 1-(3,4-dichlorophenyl)-2-(5-p-tolyl-1,3,4-oxadiazol-2-ylthio)ethanone	378.
82.	BF-III-48	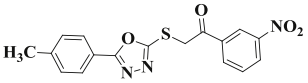 1-(3-nitrophenyl)-2-(5-p-tolyl-1,3,4-oxadiazol-2-ylthio)ethanone	355.
83.	BF-III-49	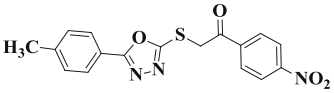 1-(3-nitrophenyl)-2-(5-p-tolyl-1,3,4-oxadiazol-2-ylthio)ethanone	355.

polar, arene cation as well as arene-arene interactions with the nitrogen atom of the 4H-pyrazole and benzene moieties of the inhibitor. Lys 155 and Phe 311 formed arene cation as well as arene-arene linkages with pyridine ring of the compound. Phe 157 and Phe 158 formed hydrophobic interactions with this compound.

Compound **4** formed four polar, 1 arene-cation, one arene-arene and one hydrophobic interaction with the active residues of the active site of the target protein as shown in Fig. 6. Arg 312 made H-bonds with the 4H-1, 2, 3-triazole moiety. Gly 159 and Asn 412 formed polar contacts with the –OH group of the compound. His 279 formed arene cation as well as arene-arene interactions with benzene moiety of the same ligand. Phe 157 formed hydrophobic contact with the ligand.

Compound **5** made three polar, one arene-cation and two arene-arene interactions with the Lys 155, Gly 159, Phe 311, Arg 312 and Asn 412 residues of the enzyme as shown in Fig. 7. Compound **6** also showed good interactions with the residues of the target enzyme, as shown in Fig. 8. This compound formed three H-bonds with the His 245, Ala 278 and His 279 residues of the protein. His 279 made arene-arene and arene cation linkage with the isoxazole moiety, while Glu 276 and Val 277 made hydrophobic linkage with the enzyme.

5. Conclusion

The molecular docking study of 1,3 4 oxadiazol compounds **1–83** were performed. The developed pharmacophore model has five important features containing two hydrogen bond acceptors (Acc), one

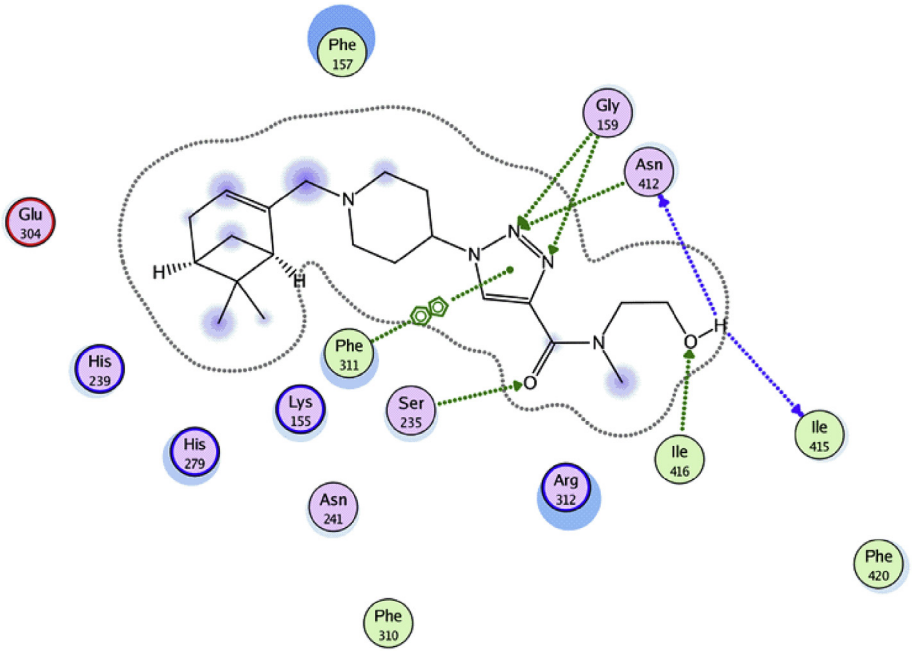

Fig. 3. 2D image showing the interaction of hit compound 1.

Don&Acc and two Hyd|Aro. A test database of 10 known inhibitors was used for the validation of the pharmacophore model, and subsequently, in database screening, it was used as a 3D query. Due to virtual screening, **37** hits (compounds) were retrieved and further following Lipinski's rule of five, **33** compounds were chosen for further evaluation by molecular docking studies. Then after docking, **10** chosen compounds were studied on the basis of the binding affinity, binding energy, docking score and protein-ligand interactions. Finally, **6** compounds of different interactions with the significant amino acid residues were selected as the lead candidates. These 6 compounds can be used as

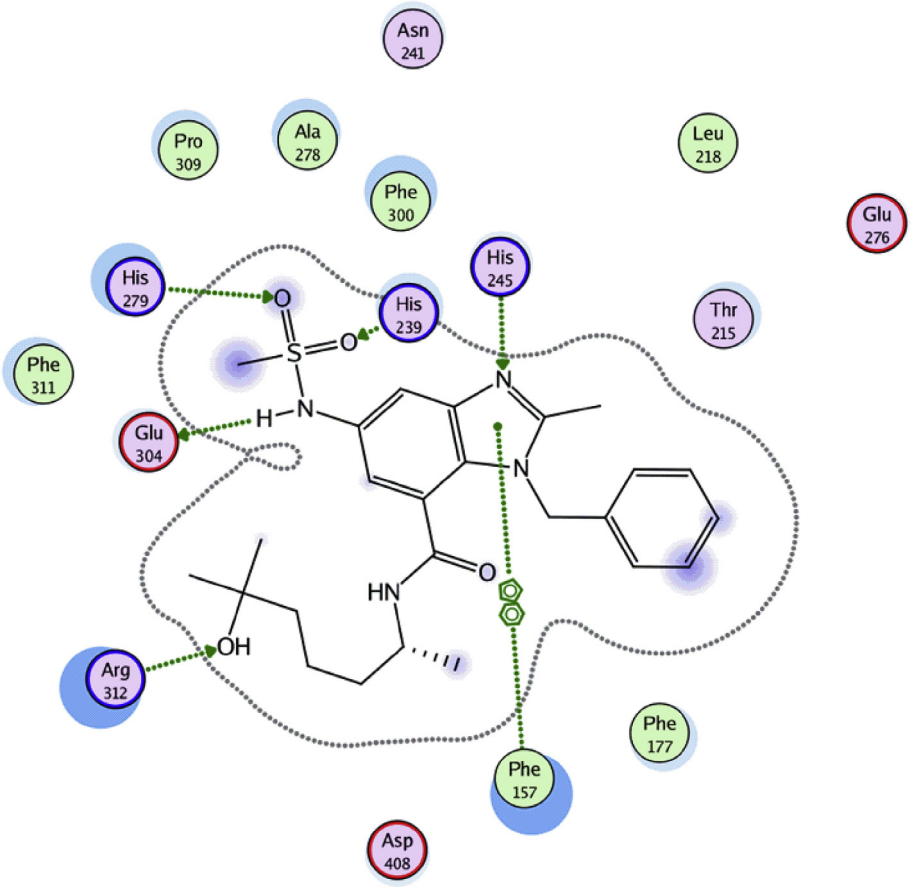

Fig. 4. 2D image showing the interaction of hit compound 2.

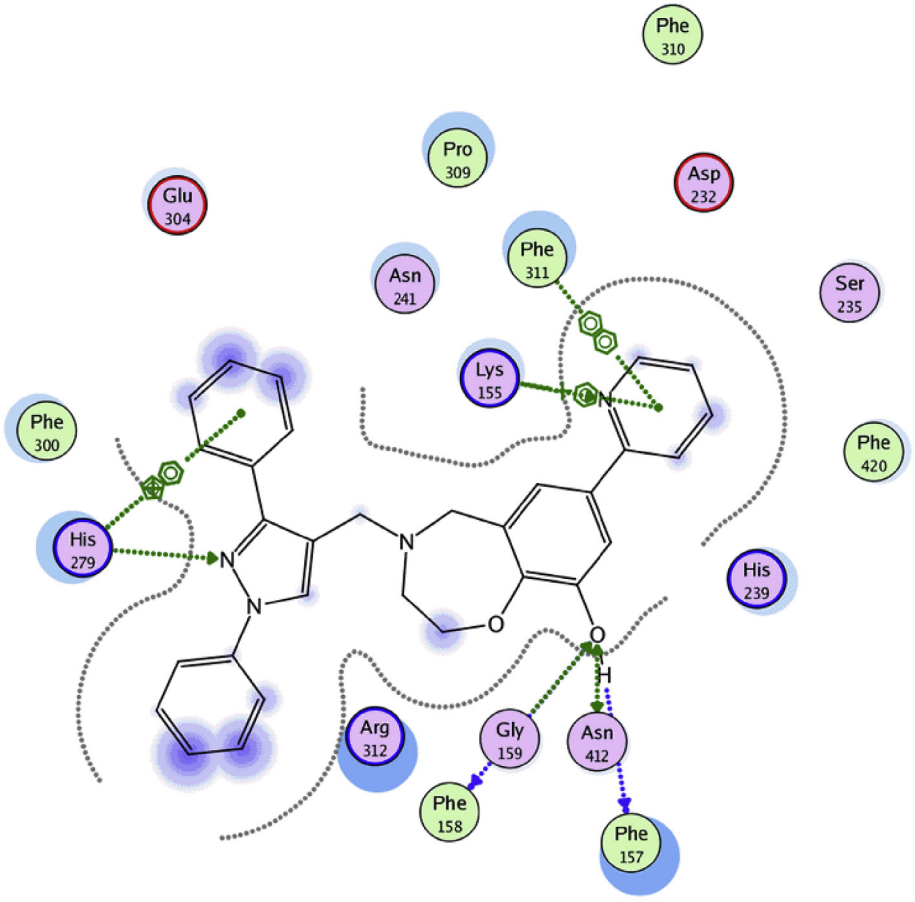

Fig. 5. 2D image showing the interaction of hit compound 3.

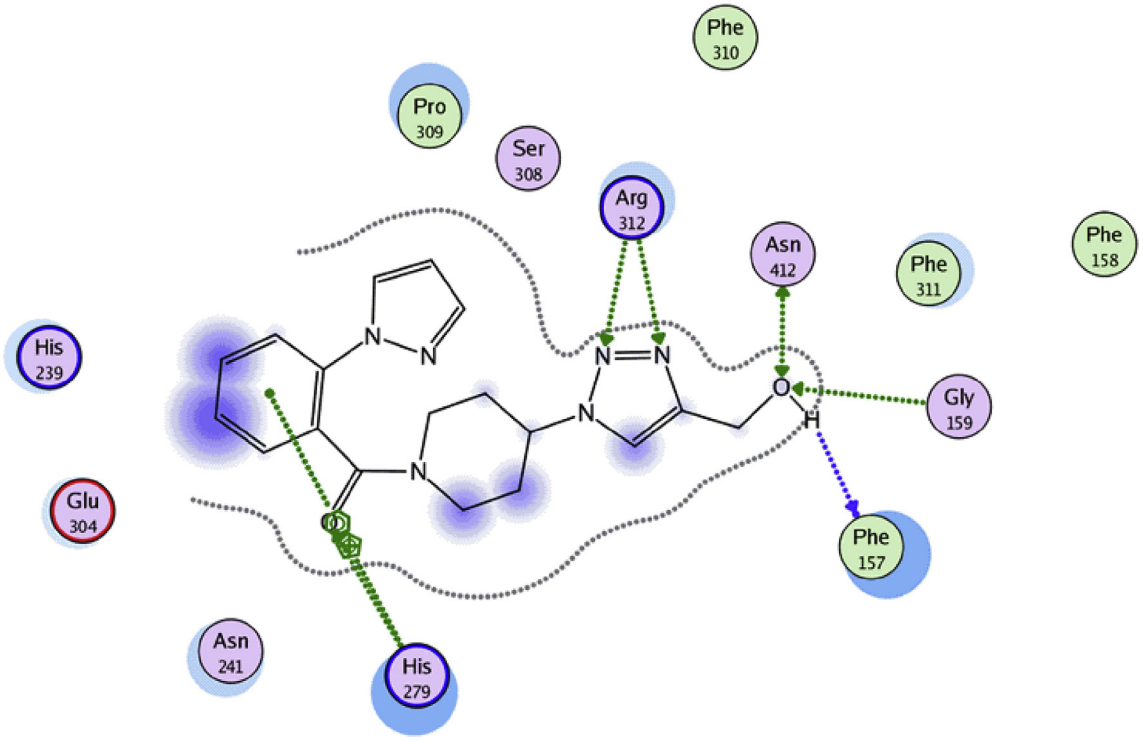

Fig. 6. 2D image showing the interaction of hit compound 4.

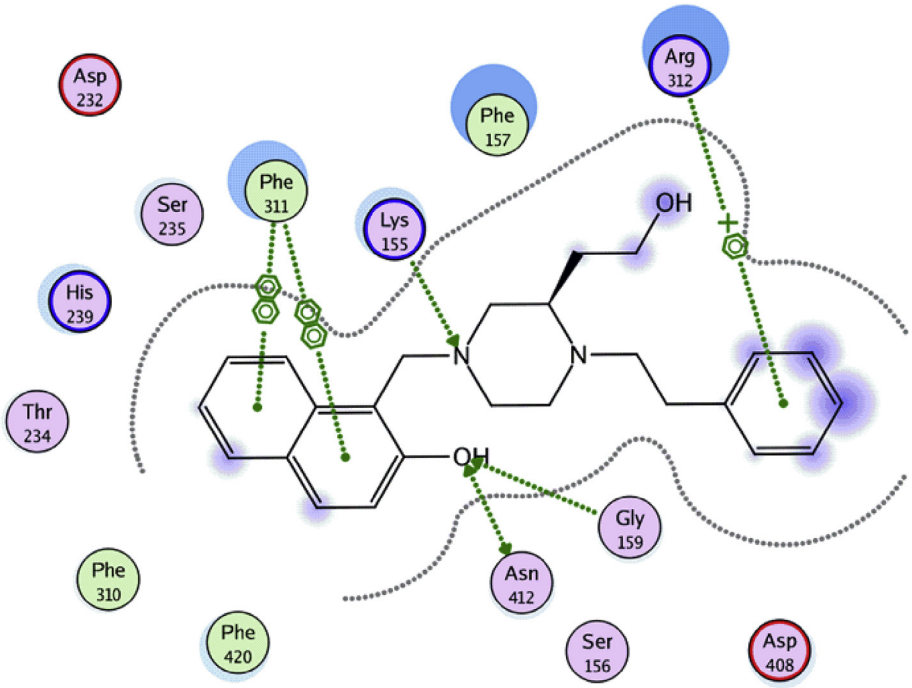

Fig. 7. 2D image showing the interaction of hit compound 5.

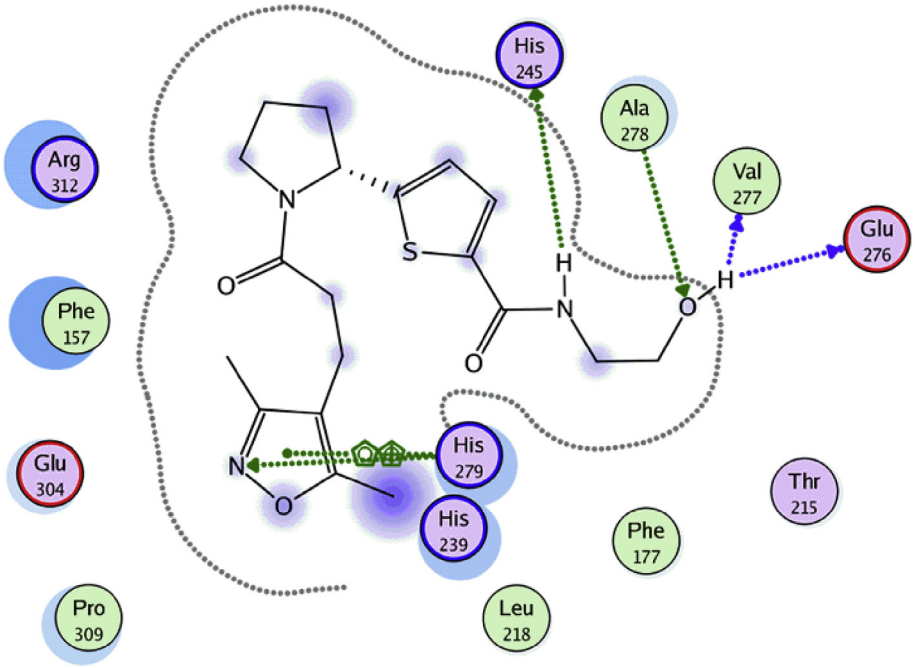

Fig. 8. 2D image showing the interaction of hit compound 6.

promising leads in the development of the novel inhibitors of drug targets, α-glucosidase enzyme.

Conflicts of interest

There is no conflict of interest in submission of this manuscript.

References

Abbas, G., Al-Harrasi, A.S., Hussain, H., 2017. Chapter 9 - α-glucosidase Enzyme Inhibitors from Natural Products A2 - Brahmachari, Goutam, Discovery and Development of Antidiabetic Agents from Natural Products. Elsevier, pp. 251–269.

Akhter, M., Husain, A., Azad, B., Ajmal, M., 2009. Aroylpropionic acid based 2, 5-disubstituted-1, 3, 4-oxadiazoles: synthesis and their anti-inflammatory and analgesic activities. Eur. J. Med. Chem. 44, 2372–2378.

Amir, M., Kumar, S., 2007. Synthesis and evaluation of anti-inflammatory, analgesic, ulcerogenic and lipid peroxidation properties of ibuprofen derivatives. Acta Pharm. 57, 31–45.

Association, A.D., 2010. Diagnosis and classification of diabetes mellitus. Diabetes Care 33, S62–S69.

Barret, R., 2018. 6 - Lipinski's rule of five. In: Barret, R. (Ed.), Therapeutical Chemistry. Elsevier, pp. 97–100.

Chandrakantha, B., Shetty, P., Nambiyar, V., Isloor, N., Isloor, A.M., 2010. Synthesis, characterization and biological activity of some new 1, 3, 4-oxadiazole bearing 2-flouro-4-methoxy phenyl moiety. Eur. J. Med. Chem. 45, 1206–1210.

Deep, A., Jain, S., Sharma, P.C., Verma, P., Kumar, M., Dora, C.P., 2010. Design and biological evaluation of biphenyl-4-carboxylic acid hydrazide-hydrazone for

antimicrobial activity. Synthesis 182, 183OC.
Derksen, S., Rau, O., Schneider, P., Schubert-Zsilavecz, M., Schneider, G., 2006. Virtual screening for PPAR modulators using a probabilistic neural network. ChemMedChem 1, 1346–1350.
Domekouo, U.L., Longo, F., Tarkang, P.A., Tchinda, A.T., Tsabang, N., Donfagsiteli, N.T., Tamze, V., Kamtchouing, P., Agbor, G.A., 2016. Evaluation of the antidiabetic and antioxidant properties of *Morinda lucida* stem bark extract in streptozotocin intoxicated rats. Pak. J. Pharm. Sci. 29, 903–911.
El-Emam, A.A., Al-Deeb, O.A., Al-Omar, M., Lehmann, J., 2004. Synthesis, antimicrobial, and anti-HIV-1 activity of certain 5-(1-adamantyl)-2-substituted thio-1, 3, 4-oxadiazoles and 5-(1-adamantyl)-3-substituted aminomethyl-1, 3, 4-oxadiazoline-2-thiones. Bioorg. Med. Chem. 12, 5107–5113.
Jha, K.K., Samad, A., Kumar, Y., Shaharyar, M., Khosa, R.L., Jain, J., Kumar, V., Singh, P., 2010. Design, synthesis and biological evaluation of 1, 3, 4-oxadiazole derivatives. Eur. J. Med. Chem. 45, 4963–4967.
Kallemeijn, W.W., Witte, M.D., Wennekes, T., Aerts, J.M.F.G., 2014. Chapter 4 - mechanism-based inhibitors of glycosidases: design and applications. In: Derek, H. (Ed.), Advances in Carbohydrate Chemistry and Biochemistry. Academic Press, pp. 297–338.
Kashtoh, H., Hussain, S., Khan, A., Saad, S.M., Khan, J.A., Khan, K.M., Perveen, S., Choudhary, M.I., 2014. Oxadiazoles and thiadiazoles: novel α-glucosidase inhibitors. Bioorg. Med. Chem. 22, 5454–5465.
Kato, A., Hayashi, E., Miyauchi, S., Adachi, I., Imahori, T., Natori, Y., Yoshimura, Y., Nash, R.J., Shimaoka, H., Nakagome, I., 2012. α-1-C-butyl-1, 4-dideoxy-1, 4-imino-l-arabinitol as a second-generation iminosugar-based oral α-glucosidase inhibitor for improving postprandial hyperglycemia. J. Med. Chem. 55, 10347–10362.
Khattak, S., Khan, H., 2018. Phyto-glycosides as therapeutic target in the treatment of diabetes. Mini Rev. Med. Chem. 18, 208–215.
Kim, S.-D., 2015. α-Glucosidase inhibitor isolated from coffee. J. Microbiol. Biotechnol. 25, 174–177.
Kitchen, D.B., Decornez, H., Furr, J.R., Bajorath, J., 2004. Docking and scoring in virtual screening for drug discovery: methods and applications. Nat. Rev. Drug Discov. 3, 935–949.
Küçükgüzel, Ş.G., Oruç, E.E., Rollas, S., Şahin, F., Özbek, A., 2002. Synthesis, characterisation and biological activity of novel 4-thiazolidinones, 1, 3, 4-oxadiazoles and some related compounds. Eur. J. Med. Chem. 37, 197–206.
Kumar, M., Verma, P., 2009. Synthesis and Antimicrobial Studies of Biphenyl-4-Carboxylic Acid 2-(aryl)-4-Oxo-Thiazolidin-3-Yl–Amide. SYNTHESIS, vol 1. pp. 1376–1380.
Kurogi, Y., Guner, O.F., 2001. Pharmacophore modeling and three-dimensional database searching for drug design using catalyst. Curr. Med. Chem. 8, 1035–1055.
Labute, P., 2008. The generalized Born/volume integral implicit solvent model: estimation of the free energy of hydration using London dispersion instead of atomic surface area. J. Comput. Chem. 29, 1693–1698.
Lipinski, C.A., Lombardo, F., Dominy, B.W., Feeney, P.J., 2012. Experimental and computational approaches to estimate solubility and permeability in drug discovery and development settings. Adv. Drug Deliv. Rev. 64, 4–17.
Lu, I.-L., Huang, C.-F., Peng, Y.-H., Lin, Y.-T., Hsieh, H.-P., Chen, C.-T., Lien, T.-W., Lee, H.-J., Mahindroo, N., Prakash, E., 2006. Structure-based drug design of a novel family of PPARγ partial agonists: virtual screening, X-ray crystallography, and in vitro/in vivo biological activities. J. Med. Chem. 49, 2703–2712.
Manjunatha, K., Poojary, B., Lobo, P.L., Fernandes, J., Kumari, N.S., 2010. Synthesis and biological evaluation of some 1, 3, 4-oxadiazole derivatives. Eur. J. Med. Chem. 45, 5225–5233.
Narayana, B., Raj, V., Kulangara, K., Ashalatha, B.V., Kumari, N.S., 2005. Synthesis of some new 2-(6-methoxy-2-naphthyl)-5-aryl-1, 3, 4-oxadiazoles as possible non--steroidal anti-inflammatory and analgesic agents. Arch. Pharm. 338, 373–377.
Nathan, D.M., Buse, J.B., Davidson, M.B., Heine, R.J., Holman, R.R., Sherwin, R., Zinman, B., 2006. Management of hyperglycemia in type 2 diabetes: a consensus algorithm for the initiation and adjustment of therapy a consensus statement from the American Diabetes Association and the European Association for the study of diabetes. Diabetes Care 29, 1963–1972.
Niaz, H., Kashtoh, H., Khan, J.A., Khan, A., Alam, M.T., Khan, K.M., Perveen, S., Choudhary, M.I., 2015. Synthesis of diethyl 4-substituted-2, 6-dimethyl-1, 4-dihydropyridine-3, 5-dicarboxylates as a new series of inhibitors against yeast α-glucosidase. Eur. J. Med. Chem. 95, 199–209.
Omar, F., Mahfouz, N., Rahman, M., 1996. Design, synthesis and antiinflammatory activity of some 1, 3, 4-oxadiazole derivatives. Eur. J. Med. Chem. 31, 819–825.
Padmavathi, V., Reddy, S.N., Reddy, G.D., Padmaja, A., 2010. Synthesis and bioassay of aminosulfonyl-1, 3, 4-oxadiazoles and their interconversion to 1, 3, 4-thiadiazoles. Eur. J. Med. Chem. 45, 4246–4251.
Reynisson, J., Court, W., O'Neill, C., Day, J., Patterson, L., McDonald, E., Workman, P., Katan, M., Eccles, S.A., 2009. The identification of novel PLC-γ inhibitors using virtual high throughput screening. Bioorg. Med. Chem. 17, 3169–3176.
Sattar, A., Abbasi, M.A., Siddiqui, S.Z., Rasool, S., Ahmad, I., 2016. Synthesis of some novel enzyme inhibitors and antibacterial agents derived from 5-(1-(4-tosyl) piperidin-4-yl)-1, 3, 4-oxadiazol-2-thiol. Braz. J. Pharm. Sci. 52, 77–85.
Scarsi, M., Podvinec, M., Roth, A., Hug, H., Kersten, S., Albrecht, H., Schwede, T., Meyer, U.A., Rücker, C., 2007. Sulfonylureas and glinides exhibit peroxisome proliferator-activated receptor γ activity: a combined virtual screening and biological assay approach. Mol. Pharmacol. 71, 398–406.
Shaikh, M., Mittal, A., Bharatam, P., 2008. Design of fructose-2, 6-bisphosphatase inhibitors: a novel virtual screening approach. J. Mol. Graph. Model. 26, 900–906.
Shyma, P., Kalluraya, B., SK, P., Synthesis, Characterization, Antidiabetic and Antioxidant Activity of 1, 3, 4-oxadiazole Derivatives Bearing 6-methyl Pyridine Moiety.
Singh, A., Sahu, V., Yadav, D., 2011. Biological activities of 2, 5-disubstituted-1, 3, 4-oxadiazoles. Int. J. Pharma Sci. Res. 2, 135–147.
Singh, P., Jangra, P.K., 2010. Oxadiazoles: a novel class of anti-convulsant agents. Chem. Sin. 1, 118–123.
Somani, R.R., Shirodkar, P.Y., 2011. Oxadiazole: a biologically important heterocycle. ChemInform 42, 130–140.
Sultan, K., Zakir, M., Khan, H., Khan, I.U., Ayaz, S., Khan, I., Khan, J., Khan, M.A., 2016a. Antihyperglycemic effect of *Persea duthieion* blood glucose levels and body weight in alloxan induced diabetic rabbits. Pak. J. Pharm. Sci. 29, 837–842.
Sultan, K., Zakir, M., Khan, H., Rauf, A., Akber, N.U., Khan, M.A., 2016b. Biofunctional properties of *Eruca sativa* Miller (rocket salad) hydroalcoholic extract. Nat. Prod. Res. 30, 1202–1204.
Testa, B., Crivori, P., Reist, M., Carrupt, P.-A., 2000. The influence of lipophilicity on the pharmacokinetic behavior of drugs: concepts and examples. Perspect. Drug Discov. Des. 19, 179–211.
Virally, M., Blicklé, J.-F., Girard, J., Halimi, S., Simon, D., Guillausseau, P.-J., 2007. Type 2 diabetes mellitus: epidemiology, pathophysiology, unmet needs and therapeutical perspectives. Diabetes Metab. 33, 231–244.
Wadood, A., Ali, S.A., Sattar, R., Lodhi, M.A., Ul-Haq, Z., 2012. A novel pharmacophore model to identify leads for simultaneous inhibition of anti-coagulation and anti-inflammatory activities of snake venom phospholipase A2. Chem. Biol. Drug Des. 79, 431–441.
Wang, L., Yan, Y.-S., Cui, H.-H., Yin, Y.-Q., Pan, J.-T., Yu, B.-W., 2016. Three new resin glycosides compounds from Argyreia acuta and their α-glucosidase inhibitory activity. Nat. Prod. Res. 31, 1–6.
Yang, X.-G., Chen, D., Xue, Y., 2012. Integration of Ligand-Based and Structure-Based Approaches for Virtual Screening of Factor Xa Inhibitors, Quantum Simulations of Materials and Biological Systems. Springer, pp. 141–154.
Yin, Z., Zhang, W., Feng, F., Zhang, Y., Kang, W., 2014. α-Glucosidase inhibitors isolated from medicinal plants. Food Sci. Human Wellness 3, 136–174.
Zafar, M., Khan, H., Rauf, A., Khan, A., Lodhi, M.A., 2016. In silico study of alkaloids as α-glucosidase inhibitors: hope for the discovery of effective lead compounds. Front. Endocrinol. 7.
Zakir, M., Sultan, K., Munir, Y., Ahmad, S., Amin, S., Khan, M.A., Khan, H., 2019. Biofunctional beverage: antihyperglycemic effect of green tea in alloxan induced diabetic rabbits. Curr. Bioact. Compd. 15, 120–124.